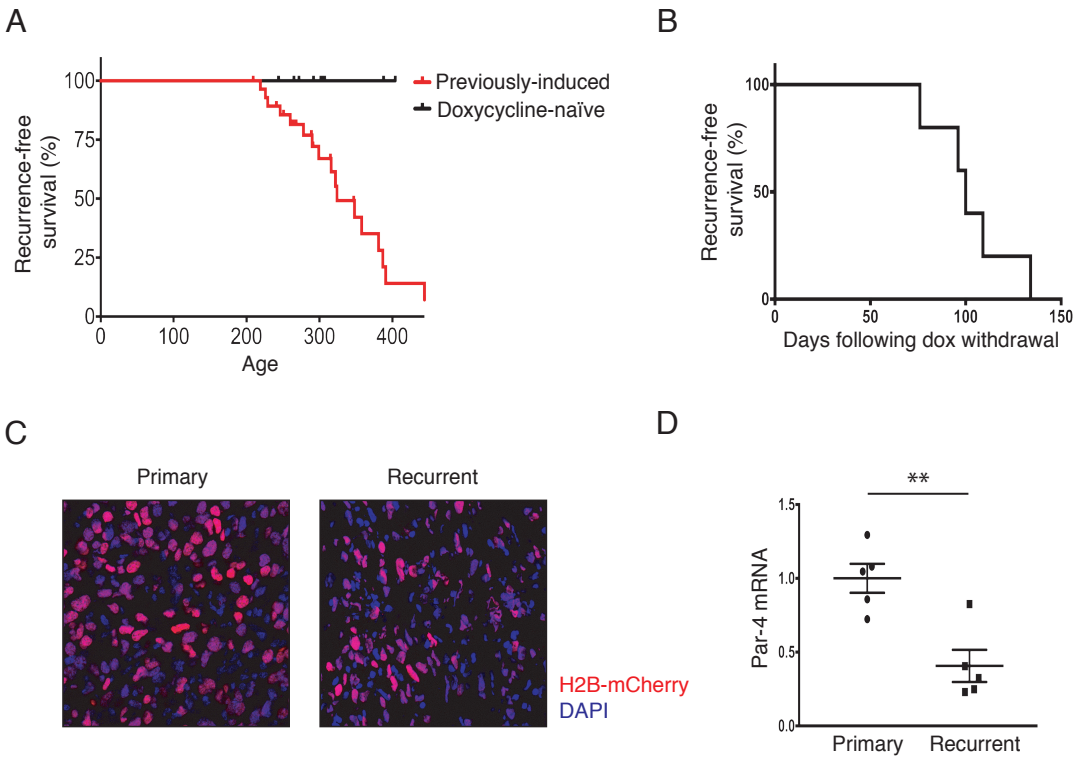

Supplemental Figure 1: Recurrent tumors are derived from primary tumors.

A. Kaplan-Meier survival plot showing recurrent tumor-free survival in mice previously induced with doxycycline (n=30) or tumor-free survival in doxycycline-naïve mice (n=10).

B. Kaplan-Meier survival plot showing recurrence-free survival following doxycycline withdrawal in a cohort of recipient mice with orthotopic tumors (n=5).

C. Representative images (40x magnification) of primary and recurrent orthotopic tumors following injection of H2B-mCherry labeled primary tumor cell line #1 into recipient mice.

D. qRT-PCR analysis of Par-4 transcripts from primary (n=5) and recurrent (n=5) orthotopic tumors. Significance determined by Student's t-test.

Error bars denote mean ± SEM. **p<0.01.

A

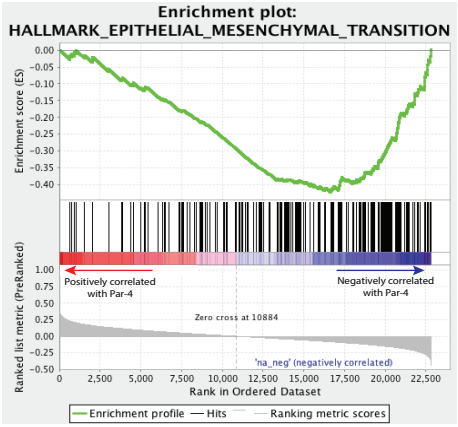

NES = -2.07335 q-value = 0.001129

B

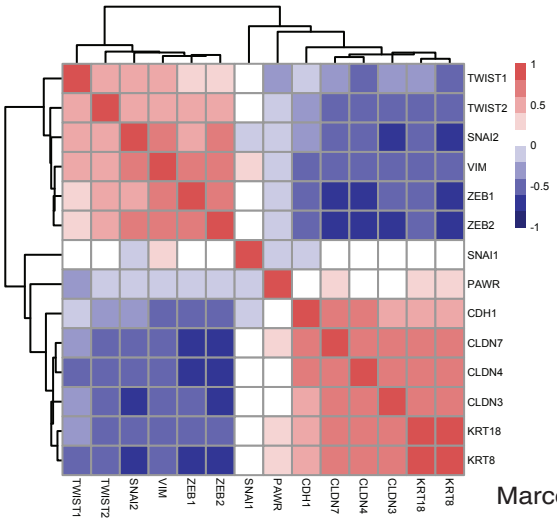

Marcotte, et al.

C

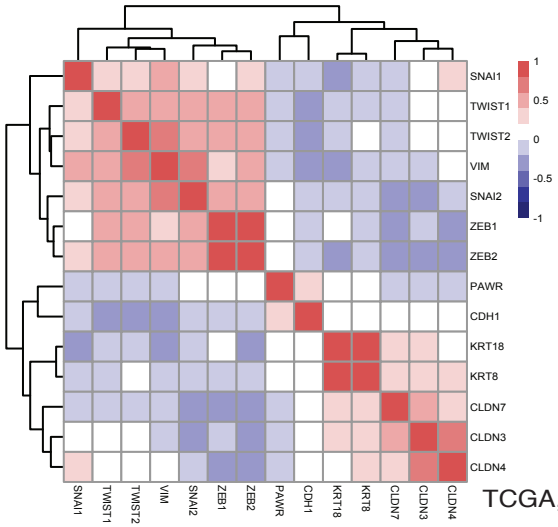

TCGA, Cell 2015

Supplemental Figure 2: Par-4 expression is negatively correlated with EMT in human breast cancer.

A. Gene Set Enrichment Analysis (GSEA) of genes associated with Par-4 expression across 86 human breast cancer cell lines. A signature for EMT was the top scoring gene set and was negatively correlated with Par-4 expression (NES=-2.07, p<0.001).

B. Heatmap showing the correlation between Par-4 expression and selected epithelial and mesenchymal markers across the 86 cell lines from (A).

C. Heatmap showing the correlation between Par-4 expression and selected epithelial and mesenchymal markers in human breast cancers from TCGA.

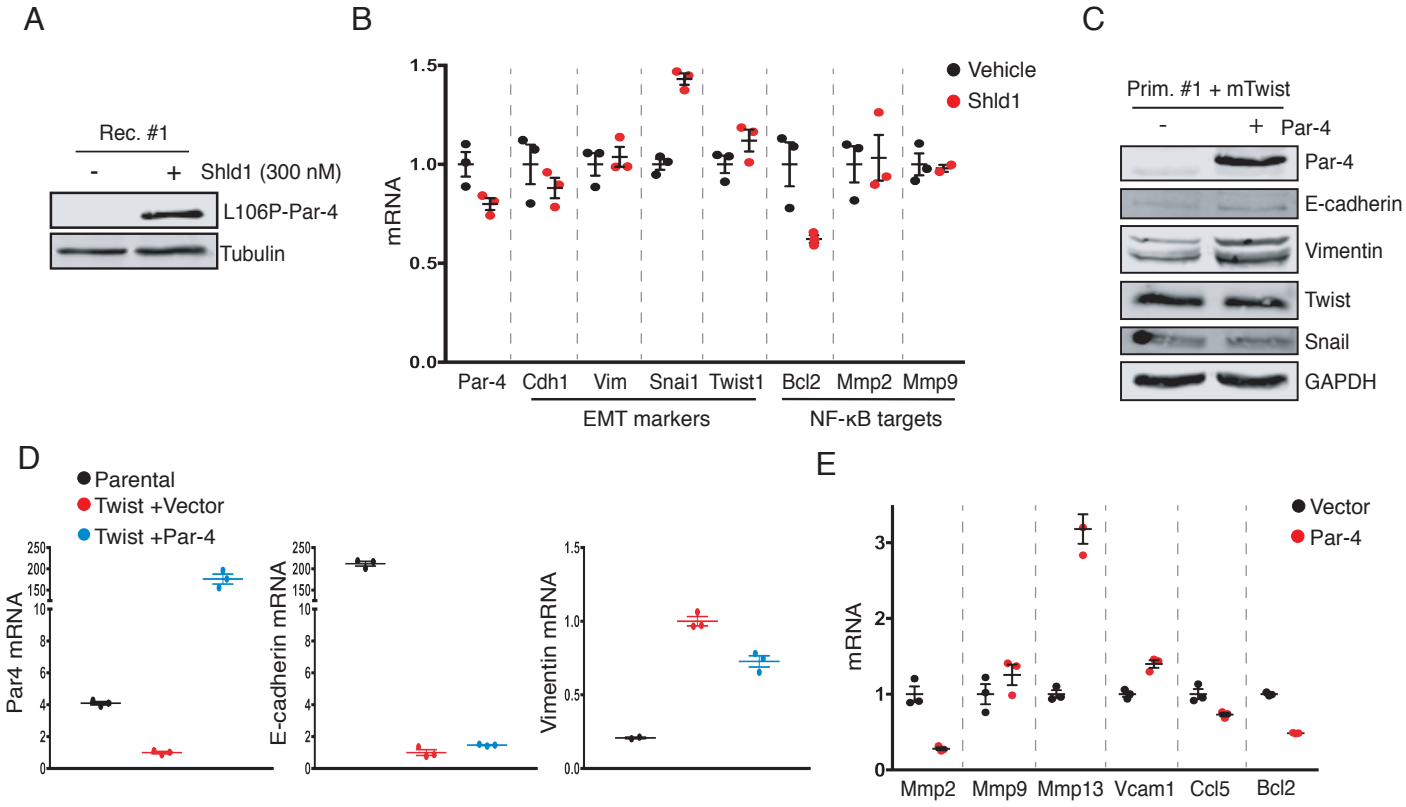

Supplemental Figure 3: Par-4 re-expression does not revert EMT or inhibit the NF-κB pathway.

A. Western blot showing Par-4 expression following 16 hours of 300 nM Shld1 treatment in recurrent tumor cell line #1.

B. qRT-PCR analysis of EMT markers (Cdh1, Vimentin, Snail and Twist) and NF-κB targets (Bcl2, Mmp2, Mmp9) in recurrent tumor cell line #1 treated with vehicle or 300 nM Shld1.

C. Western blot showing the expression of Par-4 and EMT markers E-cadherin, vimentin, Twist and Snail in Twist-transformed primary tumor cell #1 infected with either empty vector or ectopic Par-4.

D. qRT-PCR analysis of Par-4, E-cadherin, and Vimentin in parental primary tumor cell line #1, or Twist-transformed primary tumor cell #1 infected with either empty vector or ectopic Par-4.

E. qRT-PCR analysis of NF-κB targets (Mmp2, Mmp9, Mmp13, Vcam1, Ccl5, and Bcl2) in Twist-transformed primary tumor cell #1 infected with either empty vector or ectopic Par-4.

Error bars denote mean ± SEM.

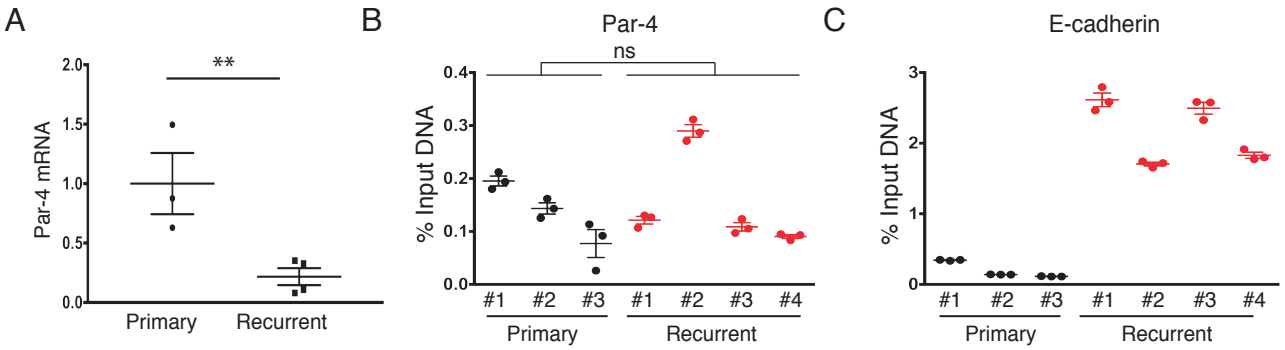

Supplemental Figure 4: H3K9me2 levels are increased at the E-cadherin promoter, but not the Par-4 promoter, in recurrent tumor cells.

A. qRT-PCR analysis of Par-4 in primary (n=3) and recurrent (n=4) tumor-derived cell lines. Significance determined by Student's t-test.

B. ChIP-qPCR analysis showing enrichment of histone mark H3K9me2 at the Par-4 promoter in an expanded panel of primary and recurrent tumor-derived cell lines. Values are normalized to input DNA.

C. ChIP-qPCR analysis showing enrichment of histone mark H3K9me2 at the E-cadherin promoter in an expanded panel of primary and recurrent tumor-derived cell lines.Values are normalized to input DNA.

Error bars denote mean ± SEM. **p-value<0.01, ns=not significant.

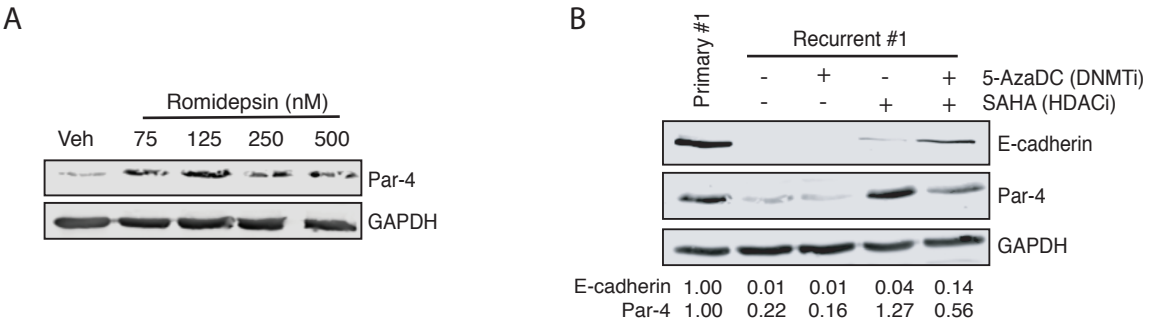

Supplemental Figure 5: Par-4 silencing in recurrent tumors can be reversed with epigenetic inhibitors.

A. Western blot analysis showing Par-4 expression following 24-hour treatment with increasing concentrations of the selective HDAC1/2 inhibitor romidepsin.

B. Western blot analysis showing Par-4 and E-cadherin expression following 48-hour treatment with vehicle, the HDAC inhibitor SAHA, or the DNMT inhibitor 5-aza-2'-deoxycytidine alone or in combination in recurrent tumor cell line #1. Primary tumor cell line #1 is shown as a control for protein expression.

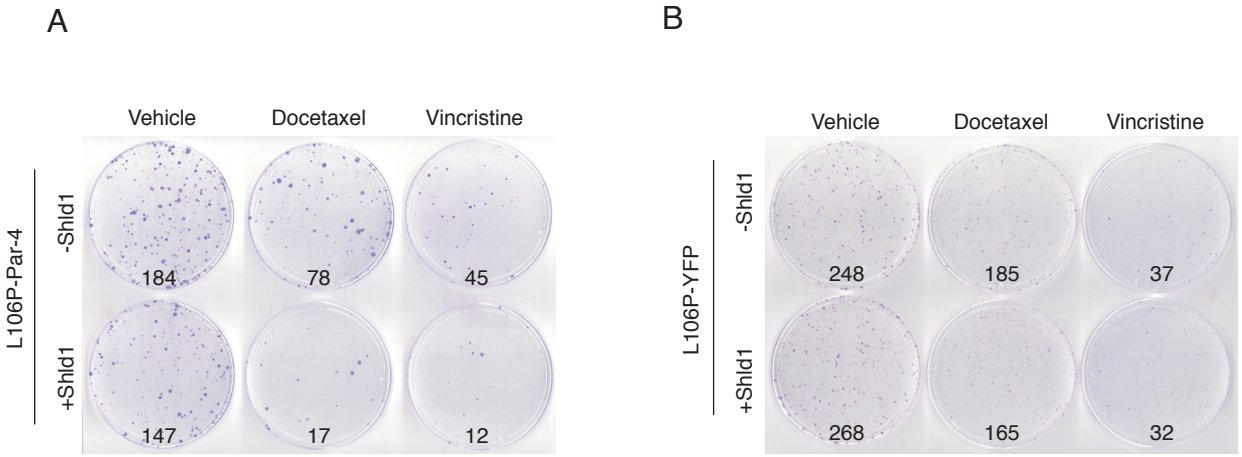

Supplemental Figure 6: Par-4 re-expression sensitizes recurrent tumor cell lines to microtubule-targeting chemotherapy drugs.

A. Colony formation assay of recurrent tumor cell line #1 expressing L106P-Par-4 and treated with either vehicle, docetaxel (20 nM) or vincristine (8 nM) along with vehicle or Shld1 (100 nM) for 8 days. Quantification of colony numbers are listed below figure.

B. Colony formation assay of recurrent tumor cell line #1 expressing L106P-YFP and treated with either vehicle, docetaxel (20 nM) or vincristine (8 nM) along with vehicle or Shld1 (100 nM) for 8 days. Quantification of colony numbers are listed below figure.

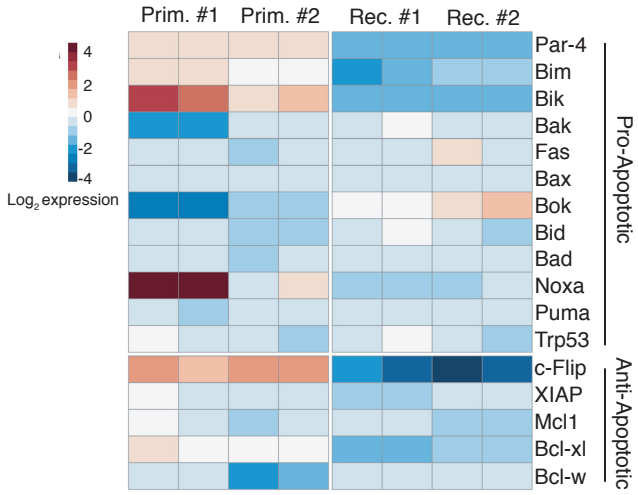

Supplemental Figure 7: Expression of apoptotic genes in recurrent tumors. Heatmap showing median-centered log_2-transformed gene expression for a panel of pro- and anti-apoptotic genes in two primary and two recurrent tumor cell lines.

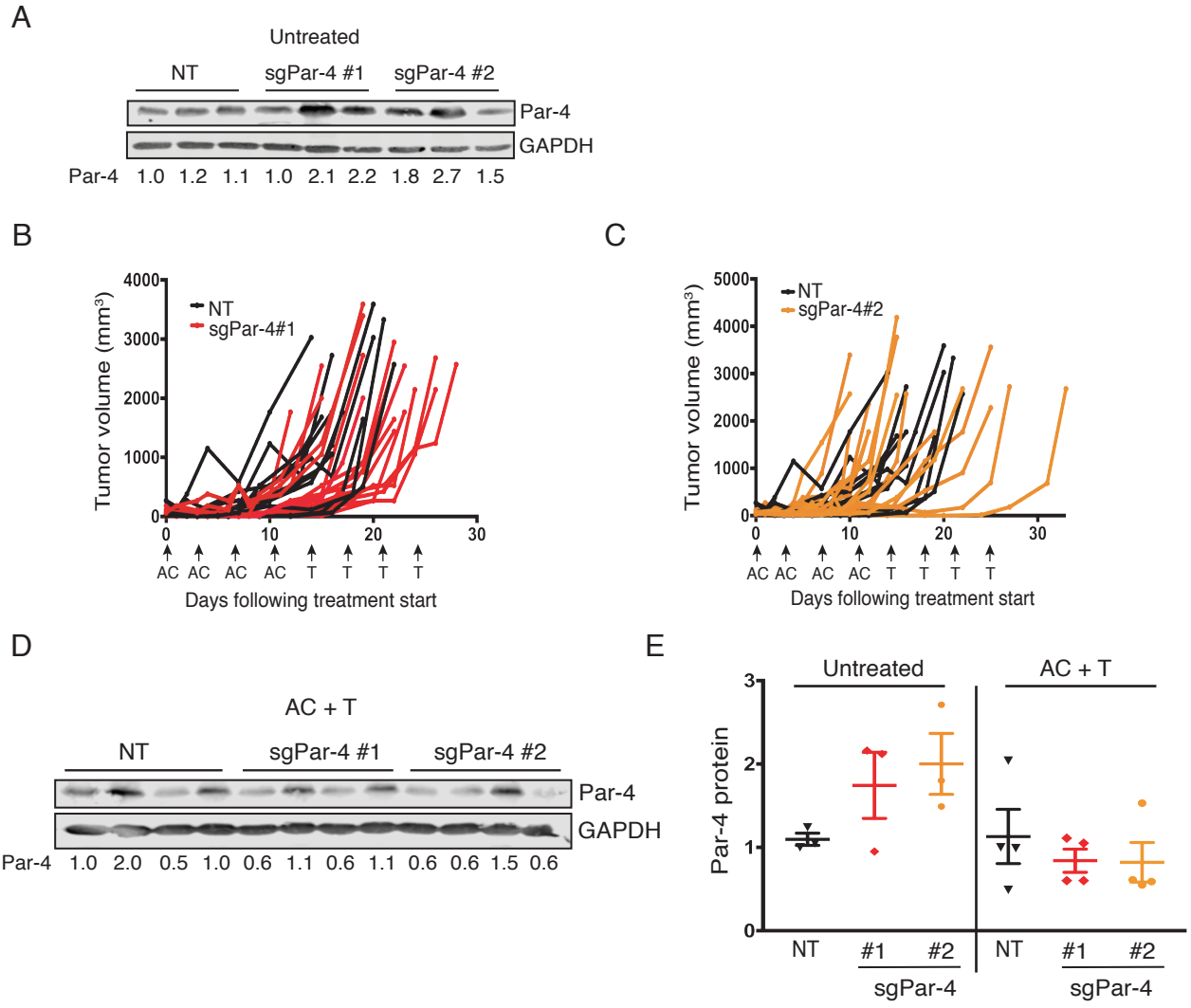

Supplemental Figure 8: Par-4 re-expression sensitizes recurrent tumors to chemotherapy in vivo

A. Western blot analysis showing Par-4 expression in untreated orthotopic recurrent tumors expressing control sgRNA, sgPar-4#1 or sgPar-4#2. Par-4 expression relative to the first lane is indicated at bottom.

B-C. Tumor growth curves for orthotopic recurrent tumors expressing a control sgRNA (NT), sgPar-4#1 (D) and sgPar-4#2 (E). Arrows indicate the days mice received chemotherapy injections. AC=Adriamycin + Cytoxan, T= Taxol.

D. Western blot analysis showing Par-4 expression at endpoint in tumors expressing control sgRNA (NT), sgPar-4#1or sgPar-4#2 and treated with chemotherapy. Par-4 expression relative to the first lane is indicated at bottom.

E. Quantification of Par-4 from panels A and D. Data are shown as normalized to the non-targeting sgRNA within each cohort.

Error bars denote mean ± SEM

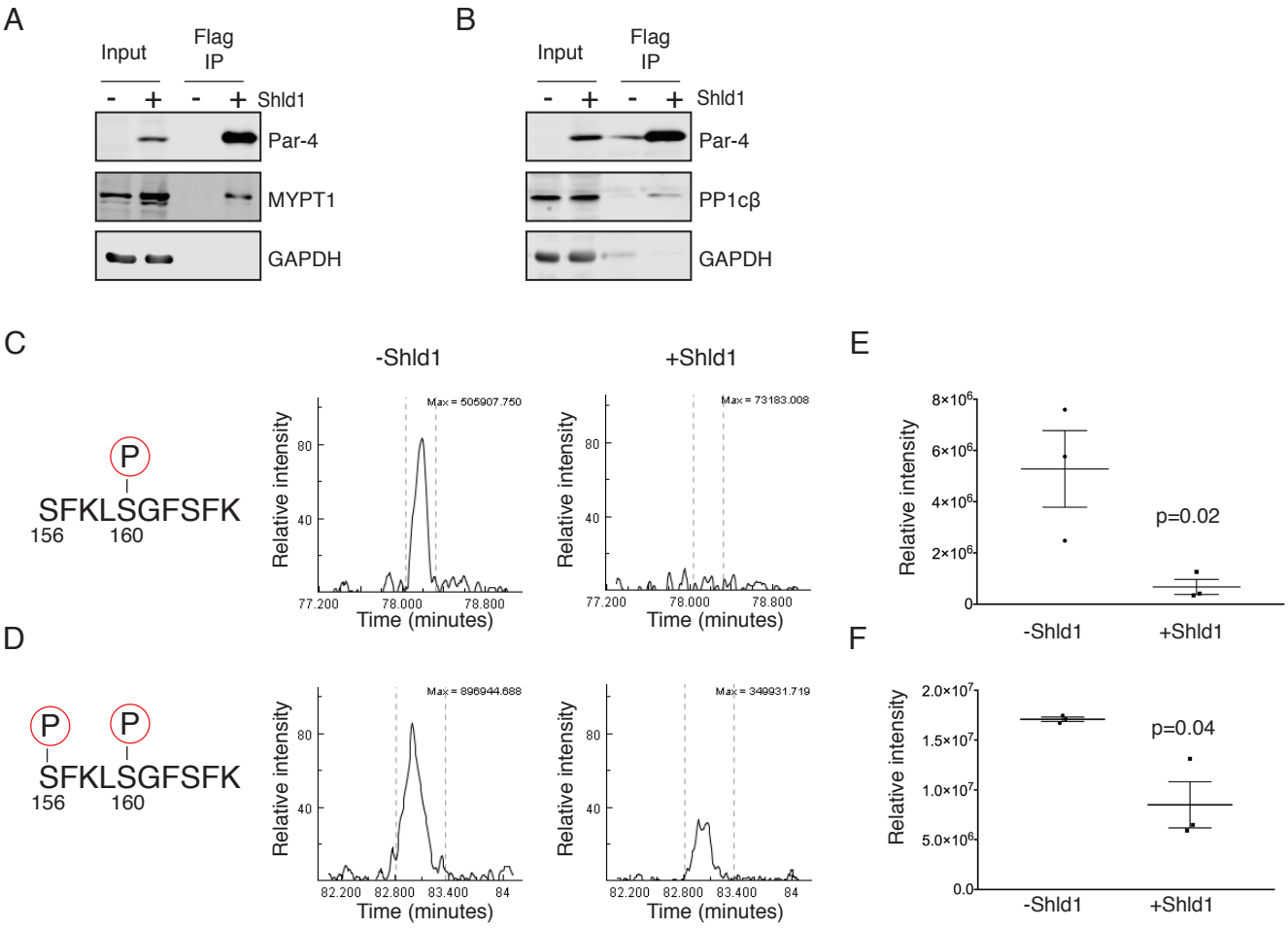

Supplemental Figure 9: Par-4 binds to PP1 subunits MYPT1 and PP1cβ and reduces MARCKS phosphorylation in recurrent tumor cells.

A.-B. Western blot analysis showing that MYPT1 (A) and PP1cβ (B) are co-immunoprecipitated with Par-4 in Shld1-treated L106P-Par-4 recurrent tumor cell line #1.

C-D. Raw data from label-free liquid chromatography-tandem mass spectrometry analysis showing the relative intensity of MARCKS phosphopeptides in vehicle and Shld1-treated recurrent tumor cell line #1. Both singly phosphorylated (Ser160) and doubly phosphorylated (Ser156/Ser160) peptides were reduced following Shld1 treatment.

E-F. Quantification of signal intensity from panels C and D. Significance determined by Student's t-test.

Error bars denote mean ± SEM.

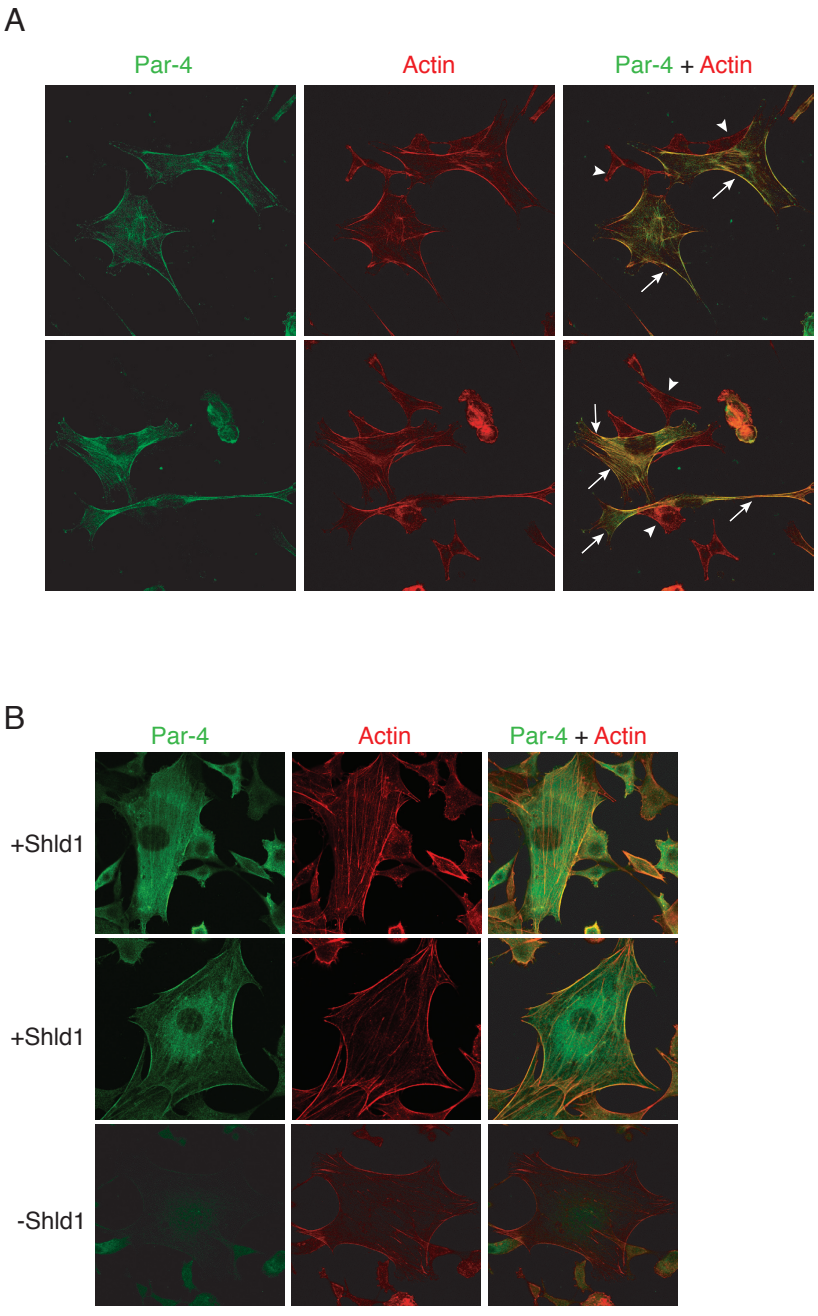

Supplemental Figure 10: Par-4 partially localizes near actin filaments in recurrent tumor cells.

A. Immunofluorescence staining for Par-4 (green) and phalloidin staining to visualize F-actin (red) in recurrent tumor cell line #1 transduced with retrovirus expressing Par-4 for 48 hours. Arrows indicate cells expressing Par-4, and arrowheads show cells not expressing Par-4. Images were captured at 63x magnification.

B. Immunofluorescence staining for Par-4 (green) and phalloidin staining to visualize F-actin (red) in recurrent tumor cell line #1 expressing L106P-Par-4 and treated with vehicle or 300 nM Shld1 for 16 hours. Images were captured at 63x magnification.

Supplemental Methods

Proteomics

Total Proteome and Phosphoproteome Analysis by Mass Spectrometry. Cell pellets were lysed in 8M Urea with 50 mM ammonium bicarbonate, normalized to protein content using a Bradford assay, reduced with DTT, alkylated with iodoacetamide, and digested with trypsin. After digestion, samples were desalted with C18 SPE then split such that approximately 10 ug was set aside for total proteome analysis and the remainder was resuspended in glycolic acid and enriched for phosphopeptides using titanium dioxide enrichment. Both the total proteome and phosphoproteome were independently analyzed using label-free differential expression LC-MS/MS on a nanoACQUITY UPLC system (Waters) coupled to a QExactive Plus high resolution accurate mass tandem mass spectrometer (Thermo). Data analysis was performed in Rosetta Elucidator with Mascot search engine.

*Mass Spectrometry Analysis of the Par-4 Interactome***.** After immunoprecipitation was complete, samples were diluted with 4x LDS loading buffer and reduced with DTT at 70°C for 10 minutes. Subsequently samples were run into a 1.5 mm Bis/Tris gel only 3 minutes at 200V and stained with colloidal Coomassie to allow for protein quantity estimation and in-gel trypsin digestion. The gel piece containing the protein was extracted with a scalpel then destained and in-gel digestion was performed using a standardized protocol (https://genome.duke.edu/sites/genome.duke.edu/files/In-gelDigestionProtocolrevised_0.pdf). Each tryptic digest was analyzed using LC-MS/MS on a nanoACQUITY UPLC system (Waters) coupled to a QExactive Plus high resolution accurate mass tandem mass spectrometer (Thermo) operating in Top10 DDA mode. Files were processed in Proteome Discover 1.4 (Thermo), searched on Mascot Server v2.5 (Matrix Sciences) using the Uniprot reviewed database with either human or mouse taxonomy. Data curation was performed in Scaffold v4 (Proteome Software, Inc).

Volcano plot to visualize phosphopeptides enrichment was produced in R (v3.3.3) with 'ggplot2' 'ggrepel' and 'dplyr' packages. Genes considered significant (p-value<0.05 and log2 fold-change > 1) were analyzed by gene ontology and dotplot was produced in R with 'clusterProfiler' (1) and 'ReactomePA' (2) packages.

Human breast cancer datasets

Quantile normalized log_2 RNAseq transcript file for 86 breast cancer cell lines were downloaded from http://neellab.github.io/bfg/ (3). The median-centered, RNA-seq transcript count expression datasets were downloaded from TCGA (4). For TCGA RNA-seq data, raw transcript counts were converted to log_2 values with a gene expression floor of -3.32. Any gene in which no sample exceeded this threshold was removed. Pairwise Pearson correlations among selected genes (Zeb1, Zeb2, Twist1, Twist2, Vim, Cdh1, Pawr, Snai1, Snai2, Krt8, Krt18, Cldn7, Cldn3, Cldn4) were determined using R (v3.3.3) software. Correlation plots for all datasets were generated with 'pheatmap' package. For GSEA analysis, genes were pre-ranked based on their correlation coefficient with Par-4 expression and input into desktop GSEA software.

Microarray analysis

RNA was isolated and purified from each of two primary and recurrent tumor cell lines in biological duplicate according to manufacturer instructions (Qiagen). Quality control for each RNA sample was evaluated prior to quantification on Mouse Genome 430A 2.0 arrays (Thermo). Microarray data was processed in R with simpleaffy (5) and limma (6) packages. Log_2 relative gene expression was median-centered and relevant pro-apoptotic genes (Par-4, Bim, Bak, Bik, Fas, Bax, Bok, Bid, Noxa, Puma, Trp53) and anti-apoptotic genes (c-Flip, XIAP, Mcl1, Bcl-xl, Bcl-w) were selected for heatmap generation with 'pheatmap' package. Microarray data were deposited in the NCBI's Gene Expression Omnibus (GEO GSE116513).

References

1. Yu G, Wang LG, Han Y, and He QY. clusterProfiler: an R package for comparing biological themes among gene clusters. *OMICS.* 2012;16(5):284-7.
2. Yu G, and He QY. ReactomePA: an R/Bioconductor package for reactome pathway analysis and visualization. *Mol Biosyst.* 2016;12(2):477-9.
3. Marcotte R, Sayad A, Brown KR, Sanchez-Garcia F, Reimand J, Haider M, et al. Functional Genomic Landscape of Human Breast Cancer Drivers, Vulnerabilities, and Resistance. *Cell.* 2016;164(1-2):293-309.
4. Ciriello G, Gatza ML, Beck AH, Wilkerson MD, Rhie SK, Pastore A, et al. Comprehensive Molecular Portraits of Invasive Lobular Breast Cancer. *Cell.* 2015;163(2):506-19.
5. Wilson CL, and Miller CJ. Simpleaffy: a BioConductor package for Affymetrix Quality Control and data analysis. *Bioinformatics.* 2005;21(18):3683-5.
6. Ritchie ME, Phipson B, Wu D, Hu Y, Law CW, Shi W, et al. limma powers differential expression analyses for RNA-sequencing and microarray studies. *Nucleic Acids Res.* 2015;43(7):e47.